International Journal on Magnetic Particle Imaging
Vol 6, No 2, Suppl 1, Article ID 2009050, 3 Pages

Infinite Science Publishing

Proceedings Article

A novel representation of the MPI system function

M. Maass[1,*] · C. Droigk[1] · A. Mertins[1]

[1]Institute for Signal Processing, Universitiy of Lübeck, Lübeck, Germany
[*]Corresponding author, email: marco.maass@uni-luebeck.de

Abstract

In a recent publication, based on the Langevin model, the exact mathematical relationship between the system function and tensor products of Chebyshev polynomials of second kind has been derived for the case in which multidimensional excitation is used for magnetic particle imaging. There, a new expression for the system function in magnetic particle imaging was derived. To make this representation easily accessible, the present paper focusses on the more practical aspects of the theory without going deep into the mathematical proofs. In particular, we examine the contribution of the mixing factors to the total energy of a system function component.

I Introduction

The mathematical formulation in magnetic particle imaging (MPI) has been subject to intensive research for several years. An overview of different models can be found in [1]. However, also for fairly simplified models, such as the Langevin function for describing the magnetization curve of superparamagnetic iron-oxide nanoparticles (SPIOs) as a function of an external magnetic field, many observations are not fully understood. A famous example is the observed relationship between tensor products of Chebyshev polynomials of second kind and the frequency components of the system function along the spatial dimension for two- [2] and three-dimensional [3] field-free point (FFP) trajectories of Lissajous type. The assumption is not a coincidence, since it was shown in [2] that for a one-dimensional FFP-trajectory the frequency components actually correspond to a convolution between the spatial derivative of the magnetization curve and weighted Chebyshev polynomials of second kind. Although this relationship is generally considered and successfully applied in practice, it has not yet been proven. Recently, we found an exact relationship between Chebyshev polynomials of second kind and the system function in terms of a series expansion [4]. However, as the series has infinite number of terms, it is not immediately clear how many terms contribute significantly to the sum. This publication summarizes the results of [4] and tries to find out how many series terms in the new two-dimensional MPI formulations are relevant.

II Known relationships

The used magnetic field in MPI is a superposition of the time-varying drive-field $\mathbf{H}^D(t)$ and the static gradient field $\mathbf{H}^S(x)$. If the gradient field is homogenous, $\mathbf{H}^S(x)$ can be described by $\mathbf{H}^S(x) = \mathbf{G}\mathbf{x}$, where $\mathbf{G}$ denotes the applied gradient strength and it is assumed to be diagonal with $\mathbf{G} = \mathrm{diag}(g_1, g_2, g_3)$. The drive-field is usually chosen as periodic trajectory $\mathbf{H}^D(t)$ with period length T_D, and for the position of the FFP we obtain $\mathbf{x}^{\mathrm{FFP}}(t) = -\mathbf{G}^(-1)\mathbf{H}^D(t)$. The voltage signal $u_l(t)$ in MPI can be represented by

$$u_l(t) = \int_{\mathbb{R}^3} s_l(\mathbf{x}, t)c(\mathbf{x})d\mathbf{x} \tag{1}$$

10.18416/ijmpi.2020.2009050

with

$$\begin{aligned} s_l(\mathbf{x},t) =& \mu_0 p_l \\ & \frac{\partial}{\partial t}\left[m\mathscr{L}(\beta\|\mathbf{G}(\mathbf{x}^{\mathrm{FFP}}(t)-\mathbf{x})\|_2)\frac{g_l(x_l^{\mathrm{FFP}}(t)-x_l)}{\|\mathbf{G}(\mathbf{x}^{\mathrm{FFP}}(t)-\mathbf{x})\|_2}\right] \\ =& \mu_0 p_l \frac{\partial}{\partial t}\left[m\mathscr{L}_l(\beta\mathbf{G}(\mathbf{x}^{\mathrm{FFP}}(t)-\mathbf{x}))\right], \end{aligned} \tag{2}$$

where $s_l(\mathbf{x},t)(l\in\{1,2,3\})$ denotes the spatial and time depending system function, the factor β reads $\beta=\frac{\mu_0 m}{k_B T}$ with μ_0 being the vacuum permeability, p_l is the inductivity of the l-th receive coil, $x_l^{\mathrm{FFP}}(t)$ denotes the l-th coordinate of the FFP, x_l is the l-th spatial coordinate, m means the magnetic moment of one nanoparticle, $c(\mathbf{x})$ is the spatial SPIO distribution, k_B is the Boltzmann constant, T is the temperature of the SPIOs, $\mathscr{L}(x)$ denotes the Langevin function and is used to describe the magnetization behavior of the SPIOs as a function of an external magnetic field, and $\mathscr{L}_l(\mathbf{x})=\mathscr{L}(\|\mathbf{x}\|_2)\frac{x_l}{\|\mathbf{x}\|_2}$ denotes the multidimensional Langevin function with respect to the l-th receive coil.

Alternatively, it is also common to write the system equation in the form of temporal Fourier series components

$$\tilde{u}_{lk} = \int_{\mathbb{R}^3} \tilde{s}_{lk}(\mathbf{x})c(\mathbf{x})d\mathbf{x}, \tag{3}$$

with

$$\tilde{s}_{lk}(\mathbf{x}) = \frac{1}{T_D}\int_{-\frac{T_D}{2}}^{\frac{T_D}{2}} s_l\left(\frac{T_D}{2},t\right)e^{-i\omega_k t}\,dt, \tag{4}$$

where $\omega_k = 2\pi k f_D$ and $f_D=\frac{1}{T_D}$.

III Fourier domain formulation of MPI

In [4], Theorem 3.1 is the most general result, which shows that the system equation of MPI can be represented in the spatio-temporal Fourier domain by

$$\tilde{u}_{lk} = \frac{\omega_k \mu_0 p_l i}{(2\pi)^3}\int_{\mathbb{R}^3}\hat{c}(\omega_{\mathbf{x}})\frac{m\hat{\mathscr{L}}_l\left(\frac{\mathbf{G}^{-1}\omega_{\mathbf{x}}}{\beta}\right)}{|\det(\beta\mathbf{G})|}P(\omega_{\mathbf{x}},k)d\omega_{\mathbf{x}}, \tag{5}$$

where $\hat{c}(\omega_{\mathbf{x}})$ and $\hat{\mathscr{L}}_l(\omega_{\mathbf{x}})$ denote the spatial 3D Fourier transform of the particle distribution and the Langevin function, respectively. The function

$$P(\omega_{\mathbf{x}},k) = \frac{1}{2\pi}\int_{-\pi}^{\pi} e^{i\omega_{\mathbf{x}}{}^T\mathbf{x}^{\mathrm{FFP}}\left(\frac{z}{2\pi f_D}\right)}e^{-ikz}\,dz \tag{6}$$

maps the spatial frequencies to temporal ones and can be evaluated for general $\mathbf{x}^{\mathrm{FFP}}(t)$. Recently, we found out that the function appears to be related to the theory of generalized Bessel functions [5,6].

IV 2D FFP Lissajous trajectory

In [4] we show that the system function for a 2D FFP-trajectory of the form

$$\mathbf{x}^{\mathrm{FFP}}(t) = \left(\frac{a_1}{g_1}\sin(2\pi f_1 t), \frac{a_2}{g_2}\sin(2\pi f_2 t), 0\right)^T, \tag{7}$$

with $f_1=\frac{f_B}{N_B}$, $f_2=\frac{f_B}{N_B-1}$, $N_B\in\mathbb{N}$, and the period length $T_D=\frac{N_B(N_B-1)}{f_B}$ can be represented by

$$\begin{aligned} \tilde{s}_{lk}(x_1,x_2) =& \sum_{\lambda\in\mathbb{Z}}\frac{(-1)^{\lambda+1}\omega_k\mu_0 p_l m\,\mathrm{sgn}(a_1g_1)\mathrm{sgn}(a_2g_2)}{\pi^2} \\ & \int_{\mathbb{R}^2}\left[\frac{\partial^2}{\partial z_1\partial z_2}\mathscr{L}_l\left(\beta\mathbf{G}\begin{pmatrix} z_1\\ z_2\\ 0\end{pmatrix}\right)\right]_{\substack{z_1=x_1-u_1\\ z_2=x_2-u_2}} \\ & V_{-k+\lambda N_B}\left(\frac{g_1}{a_1}u_1\right)V_{k-\lambda(N_B-1)}\left(\frac{g_2}{a_2}u_2\right)d\,u_1\,d\,u_2, \end{aligned} \tag{8}$$

with

$$V_n(x) = \begin{cases} \mathrm{rect}\left(\frac{x}{2}\right)\left(\frac{-U_{|n|-1}(x)\sqrt{1-x^2}}{|n|}\right) & \text{if} \quad |n|>0 \\ \frac{\pi}{2}\mathrm{sgn}(x+1)-\mathrm{rect}\left(\frac{x}{2}\right)\cos^{-1}(x) & \text{if} \quad n=0, \end{cases} \tag{9}$$

where $U_n(x)$ denotes the Chebyshev polynomials of second kind with order n. This result shows that the system function in MPI can be represented as tensor product of $V_n(x)$ convolved with a spatial derivative of the Langevin function. In contrast to the one-dimensional scenario we have an infinite series over tensor products. Fortunately, only a few series terms will make significant contribution. The exact number of important series terms depends on the parameter setting.

V Material and methods

To demonstrate how many terms in the series (8) are relevant, we have simulated the system function $\tilde{s}_{lk}(x_1,x_2)$ with the parameters given in [4] except for the particle diameter. The particle diameters were 30 nm and 40 nm. For $k\in\mathbb{Z}$, the mixing order [2] was minimized by

$$\lambda^*(k) = \mathrm{argmin}_{\lambda\in\mathbb{Z}}|k-\lambda(N_B-1)|+|k-\lambda N_B|, \tag{10}$$

because it was assumed that the most relevant terms in (8) are near to $\lambda=\lambda^*(k)$. In the experiment N_B was 32. To

identify the relevant contributing terms in (8), we derive

$$t_{\nu k}(x_1,x_2)=\frac{\omega_k\mu_0 p_l m}{\pi^2}$$
$$\int_{\mathbb{R}^2}\left[\frac{\partial^2}{\partial z_1\partial z_2}\mathscr{L}_l\left(\beta\mathbf{G}\begin{pmatrix}z_1\\z_2\\0\end{pmatrix}\right)\right] \quad \begin{aligned} z_1&=x_1-u_1\\ z_2&=x_2-u_2\end{aligned}$$
$$V_{-k+(\nu+\lambda^*(k))N_B}\left(\frac{g_1}{a_1}u_1\right)$$
$$V_{k-(\nu+\lambda^*(k))(N_B-1)}\left(\frac{g_2}{a_2}u_2\right)d\,u_1\,d\,u_2\,, \qquad (11)$$

for different $\nu,k\in\mathbb{Z}$, followed by the calculation of the ratios between the energies of (11) and (8):

$$\mathrm{relEng}_l(\nu,k)=\frac{\|t_{\nu k}\|^2_{L_2}}{\|\tilde{s}_{lk}\|^2_{L_2}}\,. \qquad (12)$$

VI Results and discussion

In Fig. 1 we show the color-coded representations of (12) for the x-receive channel ($l=1$) in the upper row with $k\in\{1,2,\ldots,2500\}$ and in the lower row with $k\in\{1,2,\ldots,100\}$. The color coding is in dB scale and truncated to the range -100 to 0 dB. In the left column, the particle diameter is 30 nm, while in the right column, it is 40 nm. It can be observed that with increasing particle diameter more terms in (11) contribute to (8). Interestingly, for $k>1500$ the λ^* calculated with (10) is no longer optimal for the first receive channel. In this case, $\nu=1$ contributes mainly to the series in (8). In the detail zoom (lower rows) it is obvious that the number of contributing terms in (8) becomes small when k is an integer multiple of $N_B-1=31$. It should be noted that with increasing k more terms contribute to the total energy. For all particle diameters tested here, however, an exponential decrease as function of ν can be observed, which shows that usually only one or two terms of (11) contribute to the total energy of (8).

VII Conclusions

We have summarized the new Fourier based MPI formulation and used the new results to examine how many series terms in (8) are relevant. We used the minimal mixing order strategy (10) to identify important components. In (10) for large k we observed a deviation for our optimization strategy, which should be investigated further in future.

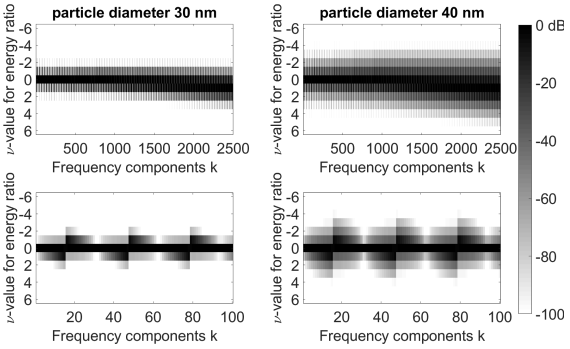

Figure 1: The color coding shows the relative energy contribution (12) of the terms in (11) relative to the energy of the system function component in (8) as function of ν and k.

Author's Statement

The author state no funding involved. Authors state no conflict of interest.

References

[1] T. Kluth. Mathematical models for magnetic particle imaging. Inverse Problems, vol. 34-8, 2018.

[2] J. Rahmer, J. Weizenecker, B. Gleich, and J. Borgert. Signal encoding in magnetic particle imaging: properties of the system function. BMC Medical Imaging, vol. 9-4, 2009.

[3] J. Rahmer, J. Weizenecker, B. Gleich, and J. Borgert. Analysis of a 3-D System Function Measured for Magnetic Particle Imaging. IEEE Trans. Med. Imag., vol. 31-6, pp. 1289–1299, 2012.

[4] M. Maass and A. Mertins. On the Representation of Magnetic Particle Imaging in Fourier Space, International Journal on Magnetic Particle Imaging, vol. 5-2, 2019.

[5] H. J. Korsch, A. Klumpp, and D. Witthaut. On two-dimensional Bessel functions. J. Phys. A: Math. Gen., vol. 39, pp. 14947–14964, 2006.

[6] G. Dattoli and A. Torre. Theory and Applications of Generalized Bessel Functions. ARACNE Rome, 1996.

